



## Partially hydrophobized catalyst particles for aqueous nitrite hydrogenation



Cristina Franch <sup>a,b</sup>, Rob G.H. Lammertink <sup>b</sup>, Leon Lefferts <sup>a,\*</sup>

<sup>a</sup> Catalytic Processes and Materials, Mesa<sup>+</sup>, Faculty of Science and Technology, University of Twente, PO Box 217, 7500AE, Enschede, The Netherlands

<sup>b</sup> Soft matter, Fluidics and Interfaces, Mesa<sup>+</sup>, University of Twente, PO Box 217, 7500AE, Enschede, The Netherlands

### ARTICLE INFO

#### Article history:

Received 6 December 2013

Received in revised form 8 March 2014

Accepted 11 March 2014

Available online 21 March 2014

#### Keywords:

Nitrite hydrogenation

Partly hydrophobized catalysts

Pd

Slurry reactor

Ammonia selectivity

### ABSTRACT

The aim of this work is to synthesize catalysts support particles that are partly hydrophobic and partly hydrophilic, with the ultimate goal to manipulate the performance of Pd supported catalysts on these supports for hydrogenation of nitrite in water. Partly hydrophobic alumina supports were successfully prepared *via* physically mixing of hydrophobic  $\alpha$ -alumina and hydrophilic  $\gamma$ -alumina, and *via* varying the amount of perfluorinated-octyltrichlorosilane (FOTS) on pure  $\gamma$ -alumina. The results from elemental analysis, SEM-EDX, XRD and contact angle measurements confirmed that the materials indeed contained hydrophobic and hydrophilic domains. Pd catalysts on supports produced *via* the mixing method resulted in a slightly increased turnover frequency as compared to the original supported Pd catalyst. Remarkably, Pd supported on partly hydrophobic alumina exhibited increased selectivity to ammonia instead of  $N_2$ , which is attributed to enhanced transfer of  $H_2$  to the active sites, *via* interaction of the catalyst particles with gas bubbles.

© 2014 Elsevier B.V. All rights reserved.

## 1. Introduction

Nitrate ( $NO_3^-$ ) excess in water is caused by fertilizers and water effluents from certain industries. Nitrate can reduce to nitrite ( $NO_2^-$ ) and its removal from water has been widely studied during the last 20 years [1–10]. The most important reason to study the removal of nitrites is its high contaminant property potentially causing cancer or blue baby syndrome [11,12]. Because of that, the European Environmental Agency (EEA) has established a legal nitrite limit in water, 0.1 mg/L for drinking water.

The nitrate and nitrite removal from water has been attempted using different techniques, including catalytic hydrogenation [13,14]. This procedure uses hydrogen as reducing agent to catalytically transform nitrite to nitrogen. Several materials have been used as catalysts supports like alumina, titania and active carbon. The catalytic active site for nitrite hydrogenation is a noble metal, either Pd or Pt, whereas nitrate hydrogenation needs addition of a less noble metal, i.e. Cu [3–10].

A disadvantage of this method is the formation of ammonia [15], which has a legal limit in water of 0.5 mg/L, as established by the EEA. The catalytic denitrification involves three phases: gas (hydrogen), liquid (water containing nitrites) and solid (catalyst).

To achieve both high activity and selectivity, proper contact between the three phases is essential. Studies related to reactor design, reaction conditions and catalyst have been presented. Most notably, membrane reactors were studied for nitrate reduction, enabling controlled hydrogen diffusion [16–18]. Optimizing hydrogen transfer to the active sites as well as increasing the hydrogen concentration will enhance the reaction rate. Unfortunately, it also results in enhanced formation of ammonia as the selectivity depends on the ratio of H-species to N-species (H/N ratio) on the active sites [4,6,8,9,19]. This ratio is determined by the local concentration of nitrite as well as hydrogen at the active sites. The challenge is to find the optimal hydrogen concentration, balancing between activity and selectivity. When reducing the hydrogen concentration to prevent ammonia formation, mass transfer limitations of hydrogen will become more dominant. Therefore, it is very important to develop catalysts and reactors that can operate efficiently at very low hydrogen concentration without significant diffusion limitation.

In this paper the synthesis of partially hydrophobized materials is presented. Such materials improve contact between the three phases, inspired on previous work by Aran et al. [20]. In that study, the authors modified a porous  $\alpha$ -alumina tube that was used as a mesoreactor. The outer part of the  $\alpha$ -alumina tube, which is in direct contact with the gas, is hydrophobized while the inner part, contacting the liquid and supporting the active Pd nanoparticles, remained hydrophilic. In this way an optimized contact is achieved

\* Corresponding author.

E-mail address: [L.Lefferts@utwente.nl](mailto:L.Lefferts@utwente.nl) (L. Lefferts).

between the gas and the liquid, minimizing diffusional distance. Although the performance of this device was not yet optimal, the achievement to manipulate the gas–liquid interface very close to the supported active sites was demonstrated at (meso-) reactor scale. Constant conversions were obtained even at very low hydrogen concentrations.

The goal of the current study is to explore a similar approach for slurry catalyst reactors, by synthesizing catalyst particles that contain hydrophobic as well as hydrophilic domains. The idea is that hydrophobic domains adhere to gas bubbles, enhancing transfer of hydrogen from the bubbles to the active sites, whereas hydrophilic domains allow efficient transport of dissolved nitrite ions. We demonstrate that manipulation of interfacial characteristics within single support particles influences conversion and selectivity in nitrite reduction.

## 2. Experimental

### 2.1. Materials

Commercial  $\alpha$ -Al<sub>2</sub>O<sub>3</sub> (Sumitomo Chemicals, 5 m<sup>2</sup>/g) and  $\gamma$ -Al<sub>2</sub>O<sub>3</sub> powder (BASF, 179 m<sup>2</sup>/g) were used as catalyst supports in this study. Palladium(II) 2,4-pentanedione (Pd(acac)<sub>2</sub>, Aldrich, 99%) in toluene (Merck, ACS) was used as catalyst precursor solution. For the surface modification steps a perfluorinated-octyltrichlorosilane (FOTS, Aldrich, 97%) and n-hexane as solvent (Sigma–Aldrich, ACS) were used as received. Sodium nitrite (NaNO<sub>2</sub>, Sigma–Aldrich, ACS) was used as source for nitrite ions (NO<sub>2</sub><sup>−</sup>) dissolved in MilliQ water.

The synthesis of particles with both hydrophilic as well as hydrophobic domains was attempted in two ways, either by mixing hydrophilic and hydrophobic particles or by partial hydrophobization of a hydrophilic sample. The first method comprises hydrophobization of  $\alpha$ -alumina, followed by mixing this material with hydrophilic  $\gamma$ -alumina; finally the mixture was pelletized and then crushed to obtain particles containing both phases. The second method was to partially hydrophobize  $\gamma$ -alumina using silanes, in one single step and using different amounts of FOTS.

### 2.2. Physical mixture of hydrophobic $\alpha$ -alumina and $\gamma$ -alumina

1.5 gram of  $\alpha$ -alumina was immersed to a 2.5 mM solution of FOTS in hexane (40 mL) for 5 min, removed from the liquid and placed in an oven at 100 °C for 1 h. After that, the sample was rinsed with hexane and dried at room temperature (adapted from [21]). FOTS is adsorbed on the surface in the first step and heating at 100 °C is aimed at improving the bonding of FOTS. The final rinsing removes the excess of FOTS which is not chemically bonded.

Pd was deposited on the  $\gamma$ -alumina surface following the subsequent recipe: the desired amount of Pd(acac)<sub>2</sub> (1 wt%) was dissolved in 40 mL of toluene. The  $\gamma$ -alumina was added and the solvent was evaporated at 50 °C. Once the sample was dried, it was placed in an oven and calcined at 250 °C during 1 h in air and then reduced at the same temperature during 2 h using a mixture of H<sub>2</sub> and N<sub>2</sub> (1:1).

0.5 g of hydrophobized  $\alpha$ -alumina was mixed in a mortar with 0.5 g of Pd/ $\gamma$ -alumina. The mixture was pressurized at 4000 bar during 1.5 min in a cold isostatic press. The pellet was broken and sieved to obtain particle sizes between 0.1 and 0.04 mm.

### 2.3. Partial hydrophobization of $\gamma$ -alumina

The Pd was first deposited on the  $\gamma$ -alumina surface following the same procedure as described in the previous section. The adsorption of FOTS was performed using 40 mL of hexane solution with different amounts of FOTS and different times for adsorption

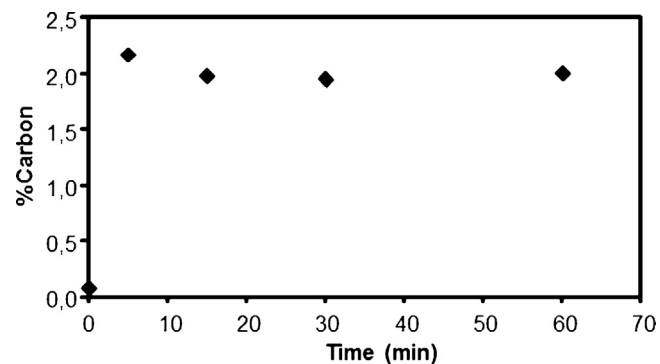


Fig. 1. Carbon weight percentage as a function of time surface modification of alumina immersed in 0.4 mmol of FOTS solution.

(0.1 mmol, 0.4 mmol, 1.6 mmol and 2 mmol of FOTS, for times varying between 5 and 180 min). As an example, for 0.1 mmol of FOTS and 5 min of adsorption: 1.5 gram of  $\gamma$ -alumina was immersed to a solution containing 0.1 mmol of FOTS in hexane (40 mL). They were kept in the solution for 5 min, taken out and placed in an oven at 100 °C for 1 h as described in the previous section. Finally, the sample was rinsed with hexane to remove any excess of silanes, and dried at room temperature.

### 2.4. Characterization

To determine qualitatively the hydrophobicity of the materials, contact angle measurements were performed on a pellet of the sample. Surface roughness of the pellet will significantly influence the contact angles, but the method allows comparison of samples and to determine the trends in the macroscopic hydrophobicity. The water contact angle was measured using an OCA 15 Dataphysics. The surface area and the pore volume were obtained from the N<sub>2</sub> adsorption isotherm obtained at 77 K (Micromeritics Tristar). X-ray fluorescence spectroscopy (XRF) was used to determine the palladium loading on the samples. CO chemisorption (Micromeritics, ChemiSorb 2750) at room temperature was used to determine the dispersion of palladium on the samples. XRD was performed using a PANalytical X'Pert-APD powder diffractometer equipped with a position sensitive detector analyzed over the 2 $\theta$ -range 5–90°. Scanning Electron Microscopy (LEO 1550 FEG-SEM) equipped with energy dispersive X-ray analysis (EDX, Thermo Noran Vantage system) was used to qualitatively study the distributions of Pd and FOTS through the material surface. Weight loss of the samples after adding FOTS was determined using thermogravimetical analysis (TGA/SDTA851e, Mettler Toledo). Elemental analysis (CHNS-O Analyzer, Interscience, Thermo Scientific) was used to determine the amount of FOTS on the surface by calculating the surface coverage of FOTS (SC) using the following equation:

$$SC \left( \frac{\text{mol FOTS}}{\text{m}^2} \right) = \%C \frac{1}{100} \frac{\text{g C}}{\text{g total}} \frac{1 \text{ mol C}}{12 \text{ g C}} \frac{1 \text{ mol FOTS}}{8 \text{ mol C}} \frac{1 \text{ g total}}{\text{BET m}^2} \quad (1)$$

where %C is the carbon-weight-concentration as obtained from the elemental analysis and BET is the surface area of the material according to N<sub>2</sub> physisorption.

The value of %C is determined by elemental analysis as a function of immersion time for the different amounts of FOTS (see Fig. 1 for an example). Experimental values for %C are obtained from the equilibrium value, which is rapidly achieved.

### 2.5. Catalytic performance

Catalytic tests were done in a stirred batch reactor at room temperature and atmospheric pressure. The reactor was glass made

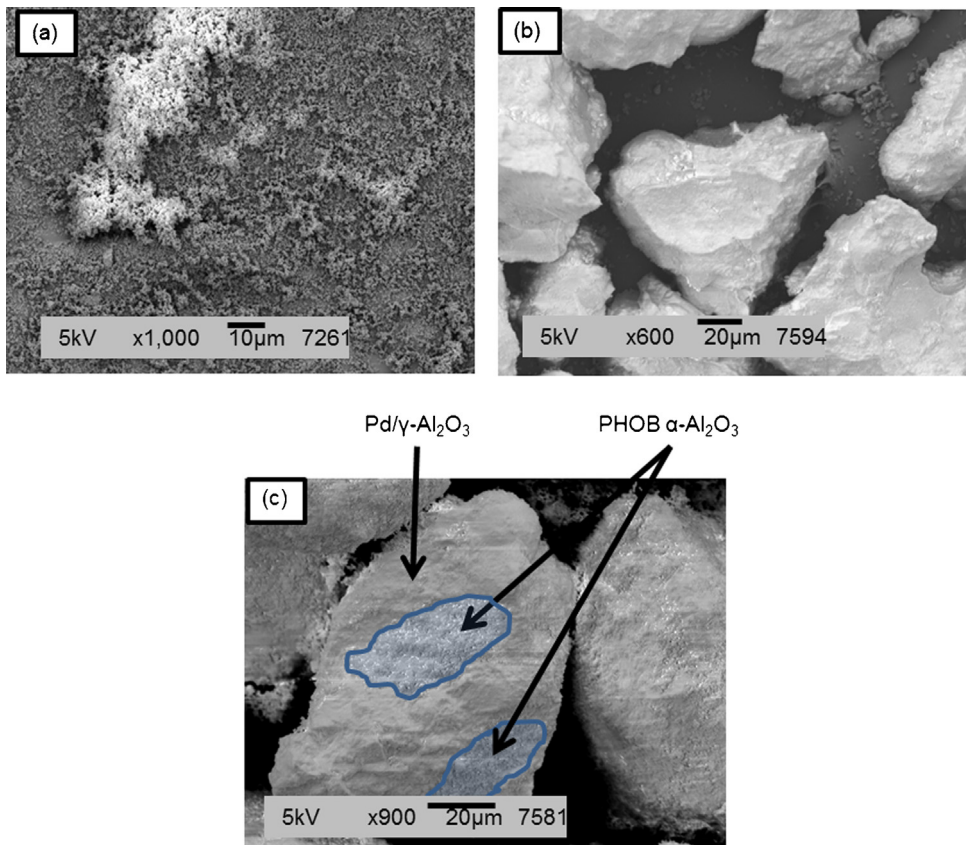


**Fig. 2.** SEM picture of: (a)  $\alpha$ -alumina; (b)  $\gamma$ -alumina; (c) physical mixture of hydrophobic  $\alpha$ -alumina and hydrophilic  $\gamma$ -alumina.

with 10 cm inner diameter and 12.7 cm height, provided with four connections on the reactor lid used for gas-in, gas-out, sampling and stirring, respectively. The glass stirrer was turbine shaped 5 cm in diameter and 0.5 cm height. 0.5 g of catalyst (sieved between 0.1 and 0.04 mm) was added to 500 mL of water containing 1,1 mmol/L of  $\text{NO}_2^-$ . The reaction was performed with 85 mL/min of  $\text{H}_2$  (1 bar of  $\text{H}_2$ ) or 10 mL/min of  $\text{H}_2$  and 75 mL/min of He (0.12 bar of  $\text{H}_2$ ) and a stirring of 1400 rpm [17,22,23].

To determine the amount of nitrites, nitrates and ammonia in the liquid phase, aliquots were taken at different reaction times and analyzed by ion chromatography (Dionex ICS-3000 DC with an UltiMate 3000 Autosampler).

### 3. Results and discussion

#### 3.1. Preparation and characterization

The amount of FOTS on the surface of  $\alpha$ -alumina was calculated using equation {1}, resulting in 4.6  $\mu\text{mol}/\text{m}^2$ . This is in reasonable agreement with 3.5  $\mu\text{mol}/\text{m}^2$  as reported in literature [24], indicating that  $\alpha$ -alumina is fully hydrophobized with this method. The hydrophobicity of the  $\alpha$ -alumina was confirmed by very low water droplet roll-off angles, representing a contact angle larger than 160°.

After that, the hydrophobicity of the sample formed by a physical mixture of hydrophobic  $\alpha$ -alumina and hydrophilic  $\gamma$ -alumina was assessed. The average contact angle measured on a pellet of this sample was 145°, i.e. the sample was partially hydrophobic. A decrease in hydrophobicity is obviously anticipated when mixing hydrophobic  $\alpha$ -alumina with hydrophilic  $\gamma$ -alumina. XRD results (not shown) confirmed that a mixture of both phases was obtained, giving distinct peaks corresponding to both the  $\alpha$ -alumina and the  $\gamma$ -alumina phases.

SEM pictures confirm that both phases can also be detected at the surface of the fabricated particles that were obtained after pressing the mixture, breaking the pellet and sieving the fraction between 40 and 100  $\mu\text{m}$ . Fig. 2a and b shows the morphology of the pure  $\alpha$  and  $\gamma$ -alumina, respectively; the small sub-micron particles of  $\alpha$ -alumina (Fig. 2a) are easily recognizable in contrast to the much larger  $\gamma$ -alumina particles (Fig. 2b). Fig. 2c clearly displays domains with both types of morphologies in the mixed material. These domains have sizes in the range of 10  $\mu\text{m}$ . Furthermore, Pd is detected exclusively in the  $\gamma$ -alumina domains, supporting the assignment of the domains with different morphologies, as  $\gamma$ -alumina is loaded with Pd whereas  $\alpha$ -alumina is not. Summarizing, physically mixing of hydrophobic  $\alpha$ -alumina and hydrophilic  $\gamma$ -alumina results in a material with both hydrophobic and hydrophilic properties.

The second approach attempts to hydrophobize  $\gamma$ -alumina partially. In this case, only  $\gamma$ -alumina was used as support and different amounts of FOTS were adsorbed. Fig. 3 represents the contact angle, the surface area and the amount of silane (SC as calculated from Eq. (1)) versus the initial concentration of FOTS (mmol of FOTS per gram of sample). This coverage is achieved after typically 5 minutes, similar to the result in Fig. 1. The surface coverage increases when increasing the amount of FOTS in the solution, reaching a constant value (3.5  $\mu\text{mol}/\text{m}^2$ ) at 1 mmol of FOTS/g sample and above. The amount of FOTS that can adsorb on the  $\gamma$ -alumina surface based on the amount of surface hydroxyl groups is 3.5  $\mu\text{mol}/\text{m}^2$  [24]. The maximum SC in Fig. 3 is in good agreement with this total amount, confirming that, full coverage with FOTS is achieved. The apparent linear increase of surface coverage as a function of FOTS amount suggests successful quantitative dosing of the silane to the surface.

The gradual increase in SC is also reflected in the contact angle measurements on pelletized samples (Fig. 3). However, the

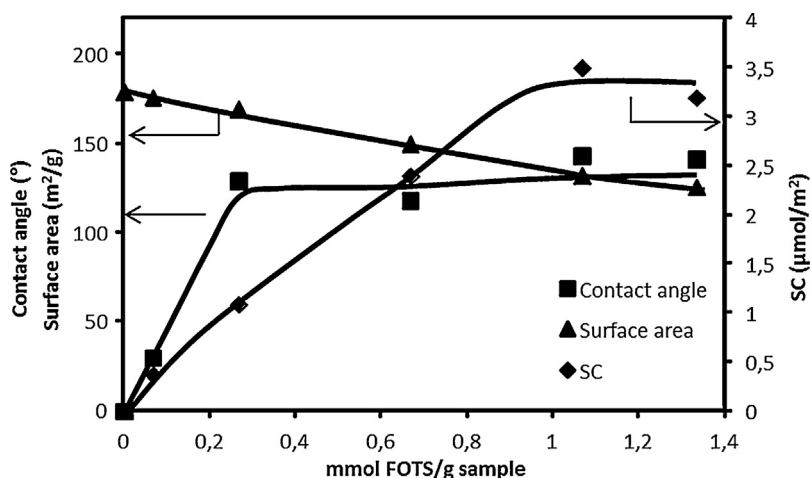


Fig. 3. Contact angle, surface area and SC by FOTS as a function of the initial amount of FOTS in the solution.

Table 1

Results from CO chemisorption of the samples tested in the catalytic reduction of nitrites.

Catalyst	Metal dispersion (%)	Metallic surface area (m <sup>2</sup> /g sample)	Metallic surface area (m <sup>2</sup> /g metal)
Pd/γ-Al <sub>2</sub> O <sub>3</sub>	57	2.7	255
Pd/γ-Al <sub>2</sub> O <sub>3</sub> + 0.02 mmol FOTS/g sample	39	1.9	175
Pd/γ-Al <sub>2</sub> O <sub>3</sub> + 0.04 mmol FOTS/g sample	38	1.8	169
Pd/γ-Al <sub>2</sub> O <sub>3</sub> + 0.1 mmol FOTS/g sample	33	1.5	148
Pd/γ-Al <sub>2</sub> O <sub>3</sub> + PHOB α-Al <sub>2</sub> O <sub>3</sub>	50	1.1	225

maximum contact angle (around 130°) is already reached at a value where the surface is partially covered with FOTS. It should be noted though, that the contact angle measurement probes the hydrophobicity of the outer surface of the pellet and that the outer surface of the pellet is formed by the outer surface of the 40–100 μm γ-alumina particles that are located at the rim of the pellet. Therefore, the results may indicate that the outer surface of the particles is preferentially hydrophobized, which would be a logical consequence of fast reaction of FOTS with the OH groups on the surface.

Obviously, if the surface reaction is fast as compared to molecular diffusion of FOTS in the pores of alumina, preferential adsorption at the outer surface is to be expected. The result in Fig. 1 indeed confirms that adsorption completes within minutes.

Fig. 3 also shows that the surface area of the sample decreases when the concentration of FOTS is increased. FOTS surface adsorption reduces the surface area available for N<sub>2</sub> physisorption or limits the accessibility of pores. Fig. 4 shows that the effect on the pore volume is much stronger though, even in the case of very low FOTS loadings.

To corroborate that the FOTS are distributed homogeneously on the γ-alumina, the sample containing 0.07 mmol FOTS/g sample was characterized by SEM-EDX (Fig. 5). Mapping of Si does not reveal any detail as compared to Al, which indicates that FOTS is homogeneously distributed on sub-micron scale. It should be noted though that the resolution is not sufficient to observe any detail on the typical length-scale of the pore size (10–20 nm). Also Pd is distributed homogeneously on this sub-micron scale. In any case, it is clear that hydrophobic domains in the order of 10 μm, as observed in Fig. 2, are absent in this sample.

The surface area of Pd was determined using CO chemisorption. The metal dispersion was calculated based on the Pd loading. As seen in Table 1, the Pd dispersion decreases with increasing amount of FOTS in the solution, indicating that FOTS is blocking part of the Pd sites, decreasing the accessibility for CO chemisorption.

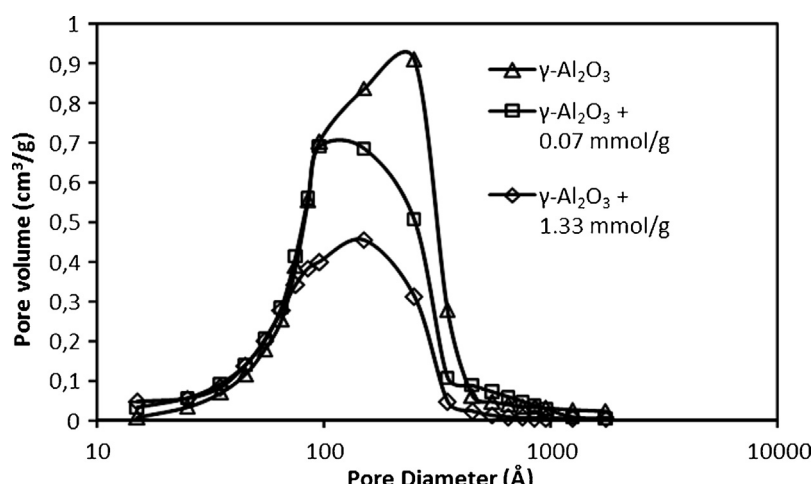


Fig. 4. Pore volume versus the pore diameter for γ-alumina, γ-alumina with 0.1 mmol of FOTS and γ-alumina with 2 mmol of FOTS.

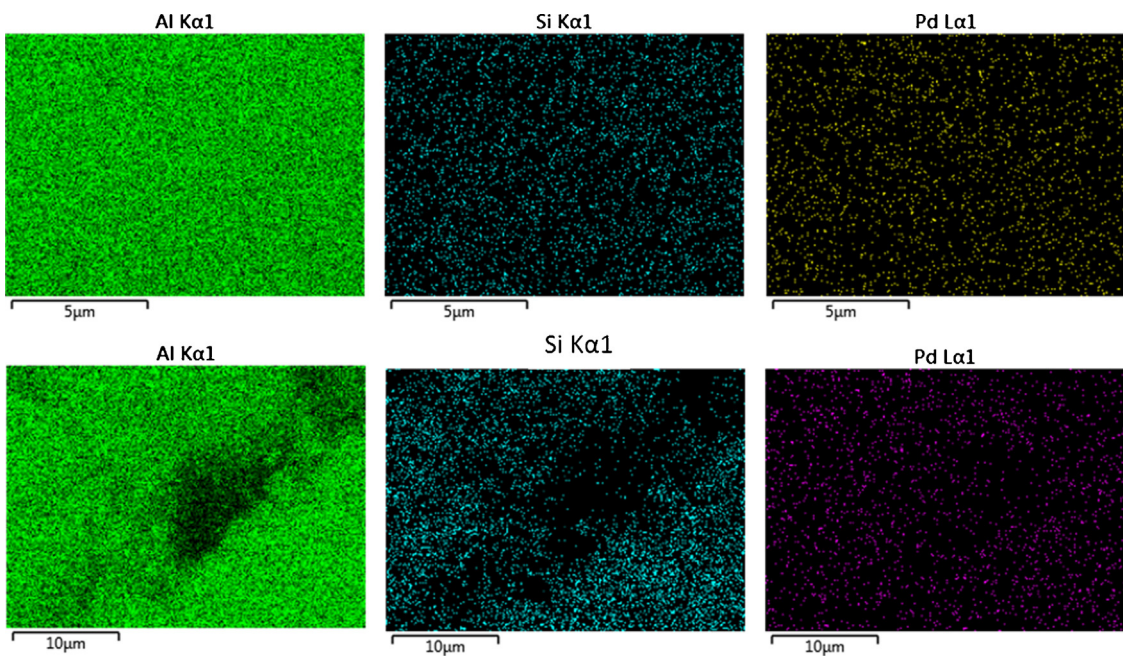


Fig. 5. Al, Si and Pd EDX analysis of the sample  $\gamma$ -alumina with 0.1 mmol of FOTS.

One can conclude that it is possible to achieve partially hydrophobic materials *via* both mixing a hydrophobic sample ( $\alpha$ -alumina) and a hydrophilic sample ( $\gamma$ -alumina) as well as dosing different amounts of FOTS to a hydrophilic sample. Based on

the apparent contact angle measured on pellets, it can be conclude that partial loading with FOTS leads to lower contact angles as compared to the mixing method. The partial loading method has the disadvantage that part of the Pd surface is affected by FOTS.

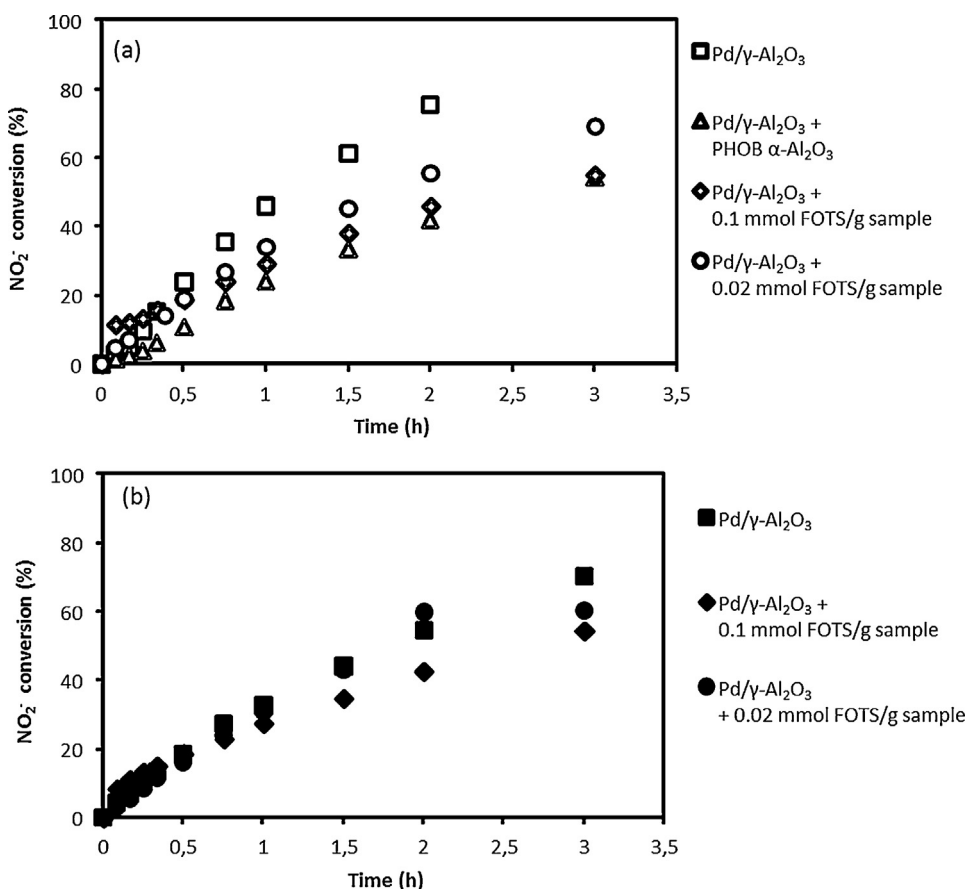
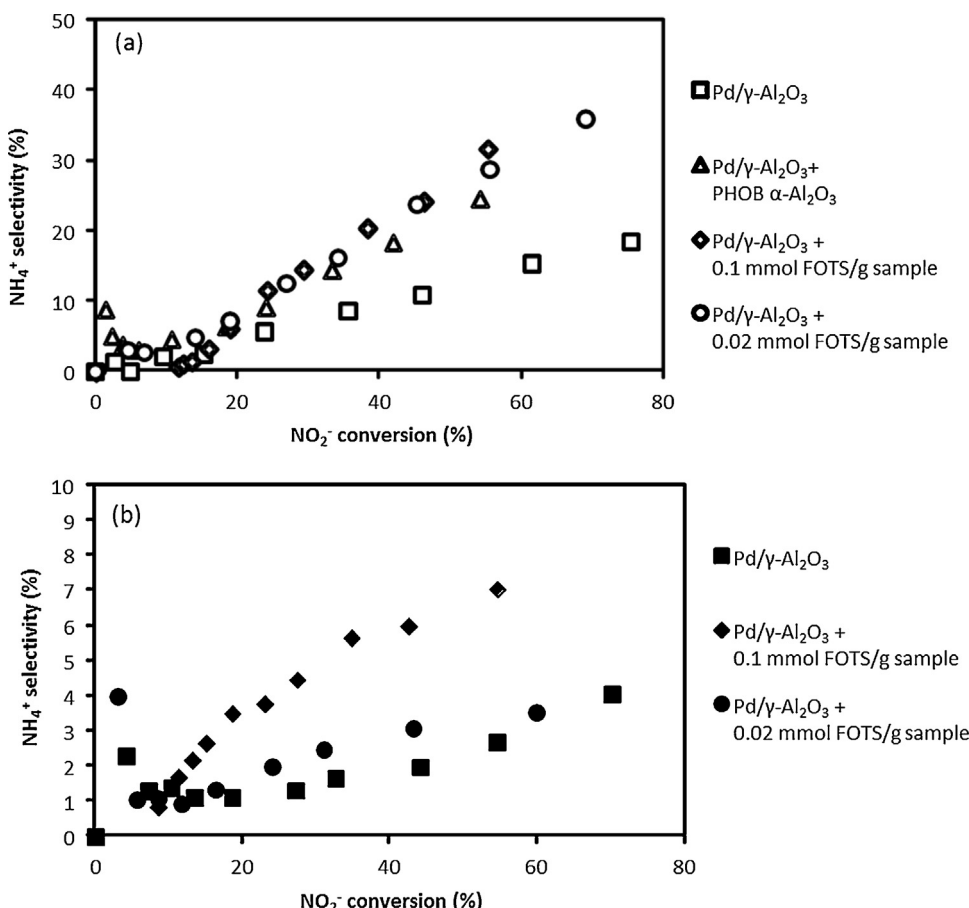


Fig. 6. Conversion of nitrites for the samples Pd/γ-alumina (□), (Pd/γ-alumina + hydrophobic  $\alpha$ -alumina) (△), Pd/γ-alumina with 0.1 mmol FOTS/g sample (◊) and Pd/γ-alumina with 0.02 mmol FOTS/g sample (○), using (a) 1 bar of hydrogen or (b) 0.12 bar of hydrogen.



**Fig. 7.** Selectivity to ammonia versus nitrite conversion for the samples Pd/γ-alumina (□), (Pd/γ-alumina + hydrophobic α-alumina) (△), Pd/γ-alumina with 0.1 mmol FOTS/g sample (◊) and Pd/γ-alumina with 0.02 mmol FOTS/g sample (○), using (a) 1 bar of hydrogen or (b) 0.12 bar of hydrogen.

### 3.2. Catalytic performance

The catalytic activity for reduction of nitrite was studied for the sample (Pd/γ-alumina + hydrophobic α-alumina) and compared to the original Pd/γ-alumina. As seen in Fig. 6a, the conversion obtained for the mixture was half the conversion obtained for the Pd/γ-alumina, at the same time of reaction and using 1 bar of hydrogen. However, the activity per mol of Pd-surface-atoms is identical within experimental error, being  $1.23 \text{ mol NO}_2^- / (\text{s mol Pd-surface})$  for the original Pd/γ-alumina and  $1.25 \text{ mol NO}_2^- / (\text{s mol Pd-surface})$  for the sample (Pd/γ-alumina + hydrophobic α-alumina). The sample formed by a mixture of both phases contains half the amount of Pd (0.5 wt%) as compared to the Pd/γ-alumina (1 wt%). Obviously, the rate of reaction scales with the amount of active phase, as was also confirmed for nitrite and nitrate reduction [25]. Apparently, manipulation of the hydrophobicity by physically mixing hydrophobic and hydrophilic samples does not affect H<sub>2</sub> transfer to such an extent that the activity of the catalyst is influenced. A detrimental affinity for the gaseous phase was observed for strongly hydrophobic samples, as floatation of the catalyst particles limited their applicability.

The catalytic activities for reduction of nitrite for 1%Pd/γ-alumina without FOTS and the samples with 0.1 mmol FOTS/g sample and with 0.02 mmol FOTS/g sample were also assessed using different partial pressures of hydrogen. As seen in Fig. 6a, the conversion of nitrites using 1 bar of hydrogen decreases for samples modified with increasing FOTS amounts. This decrease could be attributed to a decrease in the accessible Pd surface area, based on CO chemisorption. Table 2 presents the TOF's calculated

accordingly, showing less variation. Addition of 0.02 mmol FOTS/g sample induces a slight increase in TOF, whereas higher FOTS concentrations cause this effect to disappear, or even cause deactivation. In any case all these effects are minor (Table 2). Remarkably, the same trend is observed in measurements at different H<sub>2</sub> pressures, i.e. 1 bar and 0.12 bar (Table 2), confirming that the small increase in activity with low FOTS loading is significant. Also the deactivating effect of high FOTS loading is observed at both pressures, in line with further decrease in apparent activity due to floatation when hydrophobicity is further increased. Furthermore, the TOF value is only weakly influenced when varying the H<sub>2</sub> pressure between 1 bar and 0.12 bar, indicating that the apparent order in H<sub>2</sub> is close to zero.

Fig. 7 displays the selectivity to ammonia ( $\text{NH}_4^+$ ) as a function of the nitrite conversion. The selectivity to ammonia increases with conversion for all four catalysts. Two effects are likely to contribute to this increase in ammonia selectivity. First, the nitrite

**Table 2**  
Turnover frequency (TOF) calculated for the samples with or without FOTS at different hydrogen partial pressures.

H <sub>2</sub> partial pressure	Catalyst	TOF (mol $\text{NO}_2^- / (\text{s mol Pd-surface}) \times 10^3$ )
1 bar	Without FOTS	1.2
	0.02 mmol FOTS/g sample	1.3
	0.1 mmol FOTS/g sample	0.9
0.12 bar	Without FOTS	1.0
	0.02 mmol FOTS/g sample	1.2
	0.1 mmol FOTS/g sample	1.1

concentration is decreasing with time whereas the hydrogen concentration remains constant so that the H/N ratio increases, resulting in more ammonia and less nitrogen formation. Second, the reaction consumes protons, so that the pH increases with conversion. A high pH is known to favor ammonia formation [4,6].

When using different partial pressures there is a significant difference in the selectivity obtained (note that the Y axis is scaled different). The selectivity to ammonia is decreased dramatically when decreasing the hydrogen partial pressure. This results in very low ammonia concentrations below 1 ppm at 60% nitrite conversion after 3 h of reaction. The selectivity to ammonia in Fig. 7a and b is similar to or lower than values reported in literature [5,7,8,10]. In this case, the H/N decreases significantly which results in a decrease in the ammonia formation [2,26,27].

The most striking observation is that both hydrophobic catalysts exhibit significantly increased selectivity to ammonia, as compared to the original Pd/ $\gamma$ -alumina. In fact, chemical modification of the support material is known to influence both activity and selectivity [20,28–30]. The silylation of the surface enhances adherence of catalyst particles to gas bubbles, i.e. hydrogen, providing very efficient transfer of hydrogen to the active sites, i.e. palladium [20,28]. We propose that the observed increased selectivity towards ammonia is due to enhanced transport and adsorption of hydrogen with respect to nitrite, increasing the H/N ratio at the active sites, enhancing the formation of ammonia [4,19]. This indicates that the selectivity of this reaction is more sensitive to the local concentrations at the active sites, as compared to activity. Subtle changes in local concentration cause significant change in the ratio of nitrogen- and ammonia-formation, whereas reaction rate is not significantly influenced.

In short, our results support the hypothesis that introducing hydrophobic domains in the alumina support can enhance transfer of hydrogen, leading to a small increase in catalyst activity, as well as a large effect on the product distribution. Unfortunately, the dominating effect is the undesired increase in selectivity towards ammonia.

#### 4. Conclusions

It is shown that it is possible to achieve partial hydrophobization of alumina supports by using a mixture of hydrophobic  $\alpha$ -alumina and  $\gamma$ -alumina or by partial hydrophobization of  $\gamma$ -alumina. The catalytic studies using these support materials showed that the presence of FOTS on the support has only minor influence on the activity of the Pd catalysts for nitrite hydrogenation. In contrast there is an important influence on the selectivity to ammonia,

which is attributed to increased exposure of the active sites to H<sub>2</sub>. The work demonstrates that local tuning of wetting properties is a feasible way to manipulate catalytic performance.

#### Acknowledgements

Authors are grateful to B. Geerdink, K. Altena–Schildkamp, T.L.M. Velthuizen, I.G.M. Pünt and M.A. Smithers for analysis and technical support.

#### References

- [1] N. Barrabés, J. Sá, *Appl. Catal. B: Environ.* 104 (2011) 1–5.
- [2] S. Horold, K.D. Vorlop, T. Tacke, M. Sell, *Catal. Today* 17 (1993) 21–30.
- [3] M. D'Arino, F. Pinna, G. Strukul, *Appl. Catal. B: Environ.* 53 (2004) 161–168.
- [4] J.K. Chinthaginjala, L. Lefferts, *Appl. Catal. B: Environ.* 101 (2010) 144–149.
- [5] F.A. Marchesini, L.B. Gutierrez, C.A. Querini, E.E. Miró, *Chem. Eng. J.* 159 (2010) 203–211.
- [6] S.D. Ebbesen, B.L. Mojett, L. Lefferts, *J. Phys. Chem. C* 115 (2011) 1186–1194.
- [7] J.K. Chinthaginjala, A. Villa, D.S. Su, B.L. Mojett, L. Lefferts, *Catal. Today* 183 (2012) 119–123.
- [8] K. Wada, T. Hirata, S. Hosokawa, S. Iwamoto, M. Inoue, *Catal. Today* 185 (2012) 81–87.
- [9] D. Shuai, J.K. Choe, J.R. Shapley, C.J. Werth, *Environ. Sci. Technol.* 46 (2012) 2847–2855.
- [10] A. Devard, M.A. Ulla, F.A. Marchesini, *Catal. Commun.* 34 (2013) 26–29.
- [11] C.S. Bruning-Fann, J.B. Kaneene, *Vet. Hum. Toxicol.* 35 (1993) 521–538.
- [12] G. Gulis, M. Czompolyova, J.R. Cerhan, *Environ. Res.* 88 (2002) 182–187.
- [13] S.D. Ebbesen, B.L. Mojett, L. Lefferts, *J. Phys. Chem. C* 113 (2009) 2503–2511.
- [14] J. Sa, J. Montero, E. Duncan, J.A. Anderson, *Appl. Catal. B: Environ.* 73 (2007) 98–105.
- [15] J. Batista, A. Pintar, M. Ceh, *Catal. Lett.* 43 (1997) 79–84.
- [16] A.J. Lecloux, *Catal. Today* 53 (1999) 23–34.
- [17] G. Strukul, R. Gavagnin, F. Pinna, E. Modaferri, S. Perathoner, G. Centi, M. Marella, M. Tomaselli, *Catal. Today* 55 (2000) 139–149.
- [18] Y. Yoshinaga, T. Akita, I. Mikami, T. Okuhara, *J. Catal.* 207 (2002) 37–45.
- [19] X. Fan, C. Franch, A.E. Palomares, A.A. Lapkin, *Chem. Eng. J.* 175 (2011) 458–467.
- [20] H.C. Aran, J.K. Chinthaginjala, R. Groote, T. Roefols, L. Lefferts, M. Wessling, R.G.H. Lammertink, *Chem. Eng. J.* 169 (2011) 239–246.
- [21] M.J. Geerken, R.G.H. Lammertink, M. Wessling, *Colloids Surf. A: Physicochem. Eng. Aspects* 292 (2007) 224–235.
- [22] A.E. Palomares, J.G. Prato, F. Marquez, A. Corma, *Appl. Catal. B: Environ.* 41 (2003) 3–13.
- [23] O.M. Ilinitch, F.P. Cuperus, L.V. Nosova, E.N. Gribov, *Catal. Today* 56 (2000) 137–145.
- [24] R.A. van Santen, P.W.N.M. van Leeuwen, J.A. Moulijn, B.A. Arreih, *Catalysis: An Integrated Approach*, Neth. Inst. for Catalysis Research.
- [25] A.E. Palomares, C. Franch, A. Corma, *Catal. Today* 172 (2011) 90–94.
- [26] W. Gao, N. Guan, J. Chen, X. Guan, R. Jin, H. Zeng, Z. Liu, F. Zhang, *Appl. Catal. B: Environ.* 46 (2003) 341.
- [27] S. Horold, T. Tacke, K.-D. Vorlop, *Environ. Technol.* 14 (1993) 931.
- [28] A. Quintanilla, J.J.K. Bakker, M.T. Kreutzer, J.A. Moulijn, F. Kapteijn, *J. Catal.* (2008) 55.
- [29] A.R. Almeida, J.T. Carneiro, J.A. Moulijn, G. Mul, *J. Catal.* 273 (2010) 116.
- [30] A. Corma, M. Domíne, J.A. Gaona, J.L. Jordá, M.T. Navarro, F. Rey, J. Pérez-Priante, J. Tsuji, B. Mc Culloch, L.T. Nemeth, *Chem. Commun.* (1998) 2211.